Scientific Research Report

Influence of Access Cavities on Maxillary Central Incisor Fracture Resistance: Finite Element Study

Yujiang Liu, Xinyao Huang, Haoyu Ke, Xinyi Song, Xinmeng Huang, Shufen Sun *

Hospital of Stomatology, Jilin University, Changchun, PR China

ARTICLE INFO

Article history:
Received 18 January 2024
Received in revised form
26 March 2024
Accepted 8 April 2024
Available online 1 May 2024

Key words:
Computer-aided design
Endodontic cavity
Finite element analysis
Fracture resistance
Maxillary central incisor
Micro-CT

ABSTRACT

Introduction and aims: Altering the position and orientation of the root canal access cavity passway, or modifying the reduction of dentin volume, can influence the strength of dentition. This study aimed to compare the effects of different access cavities on the biomechanical performances of maxillary central incisors with a finite element analysis.
Methods: Based on the micro-computed tomography (CT) scan of a maxillary central incisor, the finite element models of the intact tooth and teeth with 4 access cavity designs: conservative incisal access cavity, incisal access cavity, conservative access cavity, and traditional access cavity were generated. Simulated occlusal forces were applied at the incisal edge of the incisor in the finite element analysis procedure.
Results: The maximum von Mises stress and maximum principal stress in the cervical area are highest in the traditional access cavity group, followed by the conservative access cavity group, incisal access cavity group, and conservative incisal access cavity group.
Conclusion: The conservative access cavities minimise the extent of dentin removal from the cervical region, protecting the mechanical behaviour of the incisor. Moving the access cavity entry point to the incisal edge also improves the fracture resistance of the incisor.
Clinical Relevance: This study's findings would help clinicians select the most appropriate endodontics access cavity method when performing the root canal on maxillary central incisors.

Introduction

The conservative endodontics access cavity has aroused great attention in the past decade. Established in 2010 by Clark and Khadeni,[1] this concept in endodontics lessens the removal of pericervical dentin with the help of 3D imaging and specialised instruments, aiming to protect the fracture resistance of the teeth. Many studies have focused on the effectiveness of conservative endodontics, including its effects on root canal cleaning and shaping, the fracture resistance of the treated tooth, and the long-term microbial reproduction in the root canal.[2-4] However, this idea of reducing the access cavity orifice has aroused some controversies as the small access may compromise the root canal treatment by impairing the location of the canal orifice and making the cleaning and shaping procedure more complicated.[5-7] Moreover, the available literature does not provide strong evidence to substantiate the claim that minimally invasive endodontic access cavities significantly enhance the fracture resistance of root-filled teeth compared to traditional access preparations.[8]

The traditional access cavity (TAC) of the incisor starts its entry point at the centre of the lingual surface. The conservative incisor access cavity has the same entrance location but a relatively smaller access cavity orifice. In the studies concerning the effect of different access cavity designs on the instrumentation of the incisor's root canal, Rover G[9] and Santos[10] performed an ultra-conservative access cavity (CAC) at the incisal ridge of the incisor crown. Another study comparing the apical centring abilities between incisal-shifted access and traditional lingual access for incisors also moved the access point to the incisal ridge.[11] Due to the lack of standardised nomenclature in the field of conservative endodontics, this type of access is referred to as the conservative incisal access cavity (CIAC) in the present study. Mauger[12] suggested

* *Corresponding author*. Hospital of Stomatology, Jilin University, 1500 Qinghua Road, Chaoyang District, Changchun 170000, PR China. (S.Sun).
E-mail address: jlussf@163.com (S. Sun).
Yujiang Liu: http://orcid.org/0009-0002-2706-3418
https://doi.org/10.1016/j.identj.2024.04.017

shifting the traditional access passway from the lingual towards the incisal region to enhance accessibility to the lingual canal and facilitate debridement. This modification could potentially resolve the issue of cingulum dentin obstructing the identification of the root canal and hindered debridement. According to the research conducted by Sarvaiya et al.,[13] an endodontic access cavity approach for incisors was developed with an entry point similar to the CIAC but with a regular-sized root canal orifice. This incisal access cavity (IAC) method has long been proposed as a good option, considering the incisor's cavities anatomy, with the potential benefit of simplifying the root canal procedure.[14-16] The alterations in tooth structure resulting from the 4 root canal treatment approaches – TAC, IAC, CIAC, and CAC – may imply different changes in the biomechanical performances of teeth. Clarifying this issue holds considerable clinical value, assisting in the nuanced assessment of the benefits and drawbacks of choosing a suitable treatment regimen that preserves the strength of patients' teeth.

There is a limited number of experiments conducted on the effects of CAC on changes in tooth structure and fracture resistance. Furthermore, the samples used, preparation methods, and storage conditions were not standardised, and there needed to be more consistency in its operational understanding and nomenclature across different studies.[5,6,9,11] Therefore, a more standardised experimental method is required to assess the effectiveness of minimally invasive techniques.[8] Therefore, our study used a finite element analysis (FEA) approach, which utilises models generated from extracted teeth to evaluate the stress distribution and peak stress levels in the tooth structure under the same simulated loading conditions. FEA reduces errors due to differences in extracted teeth and experimental operation inaccuracies.

This study aims to compare the effects of different access cavities on the biomechanical performances of incisors, aiding clinicians in selecting the most appropriate operating method. The null hypothesis is that changes in the endodontic access cavity models do not influence the maximum von Mises (VM) stress and the maximum principal stress in dentin.

Materials and methods

Micro-CT scan and model generation

This study received approval from the local ethics committee (protocol no. 202309) and was conducted strictly with the World Medical Association Declaration of Helsinki (2002 version). Before enrollment, all participants were provided with comprehensive oral and written information about the study and subsequently signed an approved written informed consent form.

Seven intact human maxillary central incisors were collected and scanned with a micro-computed tomography (CT) scanner (scanco, μCT 45, SCANCO Medical, Switzerland), resulting in 400 image slices each. The scanning parameter was set at 70 kV, 60 μA, and 600 ms using a 0.1 mm aluminium filter during the 360° rotation. The rotational step was at 0.1°, and a resolution of 10 μm was selected. Scanned image

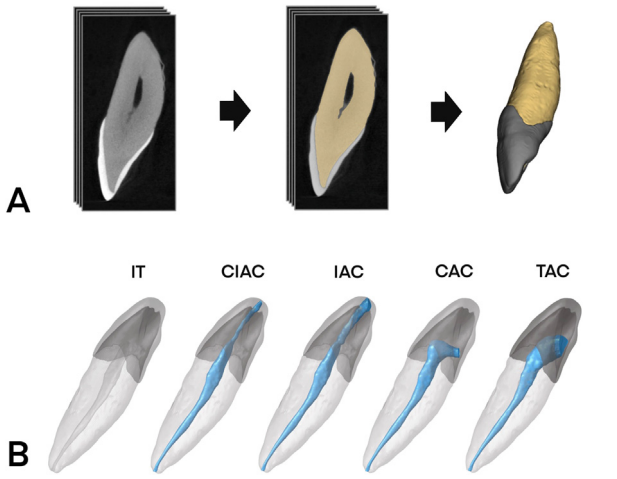

Fig. 1 – A, Illustration of extracting tooth dentin and enamel models from micro-CT scan data using the 3D Slicer software. B, Schematic diagram of the intact tooth (IT) and 4 access cavity designs: conservative incisal access cavity (CIAC), incisal access cavity (IAC), conservative access cavity (CAC), and traditional access cavity (TAC).

stacks of the specimens in DICOM format were imported to 3D slicer software (http://www.slicer.org). One specimen with a classic incisor feature was selected and used for model generation. The tooth enamel, dentin, and root canal were extracted and transferred into models using the threshold segmentation module. Smooth and solid models were generated by separately merging and fusing voxels of the extracted enamel and dentin models. Figure 1. A illustrates the process of extracting tooth dentin and enamel models from micro-CT scan data using the 3D Slicer software.

The Meshmixer software (Autodesk, San Francisco, CA, USA) was used to establish the bone and periodontal ligament models and assemble the models created above into a complete incisor model. The model of the periodontal ligament was a 0.25 mm thick layer covering the root from 1.5 mm apical to the cementoenamel junction (CEJ).[17,18] The cancellous and cortical bone models were constructed as cylinders that encircled the periodontal ligament model with thicknesses of 4 and 5 mm, respectively.[18,19]

Access cavity design and model meshing

Four access cavity passways and their corresponding composite resin restoration were designed using Meshmixer software (Figure 1B). (1) TAC: The initial entry point was positioned on the lingual surface of the dental crown, 1 mm above the cingulum. A smooth cavity pathway was created to connect the triangular-shaped entrance to the root canal orifice. The size of the access cavity orifice is approximately 3.7 mm^2; (2) IAC: The initial entry point was set between the incisal one-third of the lingual surface and the incisal ridge. The opening was designed to be an oval cavity extending from the incisal ridge to the centre of the lingual surface. The size of the access cavity orifice is approximately 3.5 mm^2; (3) CAC: The entry point was set at the lingual surface of the dental crown, with the cavity entrance designed to be minimally

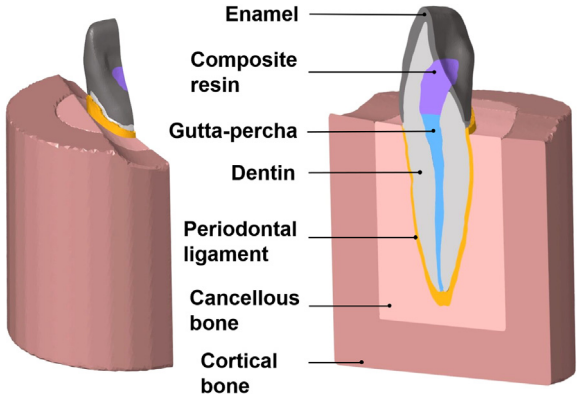

Fig. 2 – Schematic diagram of the finite element analysis (FEA) model.

invasive to preserve the pericervical dentin. The size of the access cavity orifice is approximately 1.7 mm^2;(4)CIAC: The starting point was positioned at the incisal edge, with a small triangular-shaped cavity created and minimally expanded to preserve the cingulum and part of the pulp chamber roof. The size of the access cavity orifice is approximately 1.6 mm^2.

The simulated root canal cleaning procedure was carried out by shaping and smoothing the extracted root canal model from the apical foramen to the CEJ. After that, the amount of removed dentin volume was calculated using the following formula: $V_{\text{intact tooth dentin}} - V_{\text{treated tooth dentin}}$, and the amount of removed pericervical dentin volume was calculated using the following formula: $V_{\text{intact tooth pericervical dentin}} - V_{\text{treated tooth pericervical dentin}}$. The pulp chamber and cavity were then filled consistently and seamlessly using the gutta – percha and composite resin model established via boolean operations in Meshmixer software (Figure 2).

All the models were then imported into Hypermesh software (Altair, Troy, MI, USA) for finite element meshing. The 3D tetra mesh and smooth pyramid module were used to construct linear tetrahedral elements within the models. After conducting convergence analysis, the element size was determined, and the number of elements ranged from 516,894 to 525,849. The 3D meshing of the models was outputted in input format for finite element analysis.

Finite element analysis

Abaqus (SIMULIA, Vélizy-Villacoublay, France) was used for the finite element analysis of the restored tooth models. The dental structures were presumed to be homogeneous, isotropic, and exhibit linear elastic behaviour. Table 1 displays the material properties of each tooth structure, utilising previously reported values from published studies.[20–26] Using the Find Contact Pairs tool in the Abaqus constraint manager, the contact surface pairs of the tooth models were automatically identified and configured as frictionless contacts, forming a composite incisor model where distinct parts possessing different material properties were seamlessly attached to one another.

The loading scenario was selected according to the typical biting situation.[27] A coordinate system was established with the x-axis along the incisal edge and the z-axis as the tooth's long axis. Two loads were selected, 250 N and 50 N, to represent the greater biting forces and the typical daily masticatory forces, respectively.[18,27,28] The load was applied at the incisal edge of the crown with an angle of 135° to the longitudinal axis of the tooth, targeting an area near the lingual side of the incisal edge, which is a simulation of incisor contact in Class I occlusal relationship.[9,29] This applied load was distributed over an elliptical area of 3.5 mm^2, as illustrated in Figure 3. In establishing the boundary conditions, the bottom surfaces of the cortical bone models were restricted in all 6 degrees of freedom.

Table 1 – Mechanical properties of the materials for finite element analysis.

Material	Elastic modulus (MPa)	Poisson's ratio
Dentin	18,600	0.31[20]
Enamel	84,100	0.33[21]
Periodontal ligament	68.9	0.45[20]
Cancellous bone	1370	0.30[22]
Cortical bone	13,700	0.30[22]
Gutta – percha	0.69	0.45[23]
Composite resin	12,000	0.30[24]
acrylic resin	2400	0.35[25]
ABS resin	2020	0.36[26]

Finite element model validation

The incisor selected from 7 extracted teeth for finite element modelling was used to validate the reliability of the FEA. An experienced endodontist, who had not observed the micro-CT images of this tooth, performed TAC on this incisor. The access cavity started at the crown's lingual surface central

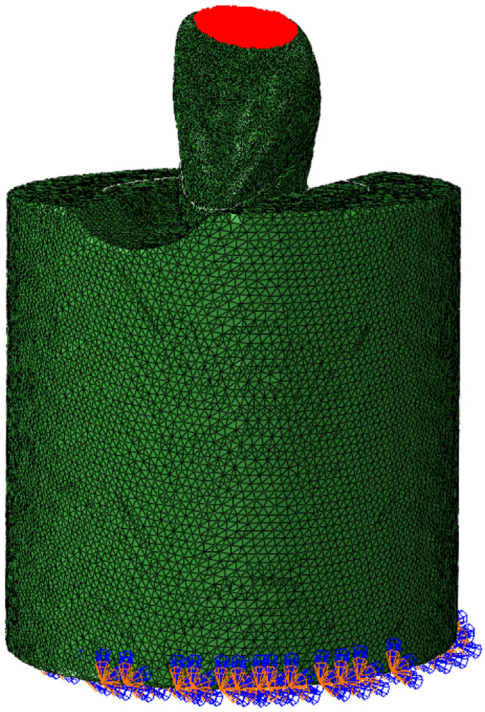

Fig. 3 – Schematic diagram of the distribution area of the FE load.

fossa, and a round bur was used to drill vertically into the lingual surface. Upon reaching the enamel-dentin junction, the direction was altered to align with the tooth's longitudinal axis. The opening of the access cavity was made into a rounded triangle, and the top of the pulp chamber was wholly removed. Subsequently, a K-file size 10 (Dentsply, Konstanz, Germany) was employed to explore the root canal all the way to the apical foramen, determine its length, and then calculate the working length by deducting 1 mm from the measured length. The root canal was then irrigated with a syringe containing 1% NaOCl solution. A K-file of size 15 was utilised to negotiate the canal, followed by the preparation of the canal with Protaper rotary files (Dentsply, Konstanz, Germany) at 250 rpm and 2.0 torque until the working length. Irrigation was performed with 2 mL of NaOCl solution following each file exchange, and upon completing the root canal's preparation, it was further rinsed with 5 mL of 17% ethylenediaminetetraacetic acid.

Following the micro-CT scan, root canal filling was performed for the tooth. A 0.6 taper gutta – percha cone (Dentsply, Konstanz, Germany) and AH Plus sealer (Dentsply, NC, USA) were used for apical closure, followed by filling the middle and upper sections of the root canal with a gutta core obturator. After filling, an alcohol-soaked cotton ball was employed to cleanse the pulp chamber, removing the filling material remnants. The enamel then underwent etching for 15 seconds, followed by rinsing and air-drying. Next, a bonding agent (3M ESPE, St Paul, MN, USA) was applied and light-cured for 10 seconds. Subsequently, the composite restoration (3M ESPE, St Paul, MN, USA) was applied, ensuring that the thickness of each layer was less than 2 mm, and each layer was cured for 40 seconds. After the root canal treatment, the tooth underwent a second micro-CT scan with the same scanning parameters as before.

The incisor was secured within a rectangular block of acrylic resin (15 × 15 × 43 mm), ensuring the portion below the tooth's CEJ was wholly embedded. The height from the top surface of the block to the highest point of the exposed tooth crown's incisal edge was measured to prepare for subsequent modelling. A pressure testing base was modelled according to the block's dimensions. The testing base was then printed using acrylonitrile butadiene styrene resin on an Ultimaker 2+ 3D printer (Ultimaker, Utrecht, The Netherlands) with the following settings: slice height of 0.1 mm, extrusion width of 0.4 mm, and a liquefier temperature of 235 °C. The block was firmly inserted into the testing base designed to fit its size, which tilted the tooth to secure it at a 45° angle on the horizontal plane. This prepared test sample was mounted horizontally on the test bench of the universal testing machine (Shimadzu, Tokyo, Japan). The square-shaped load cell exerted pressure onto the lingual surface of the teeth at a velocity of 1 mm/min, increasing the force from 0 N to 250 N. (Figure 4A) The machine recorded the vertical deformation of the test sample with a precision of 0.00001 mm under forces of 25 N, 50 N, 75 N, 100 N, 125 N, 150 N, 175 N, 200 N, 225 N, and 250 N.

Using microCT data from the second scan, the same methodology was applied for modelling and meshing of the tooth's dentin, enamel, gutta – percha, and composite resin. These models were assembled with the block model and the testing base model. (Figure 4B) All models were imported into Abaqus software to simulate the deformation condition of the sample under forces of 25 N, 50 N, 75 N, 100 N, 125 N, 150 N, 175 N, 200 N, 225 N, and 250 N. The models' contact methods, boundary conditions, and other parameters matched those used in FEA. The material properties of the self-curing acrylic resin block and acrylonitrile butadiene styrene resin testing base were determined from published studies and listed in Table 1. The direction and application point of the simulated forces coincided with those in the universal testing machine experiment, angled at 45° to the tooth's long axis. The force was applied to an area that matched the load cell's projection on the lingual surface of the crown (7.2 mm^2). A coordinate axis was established during Abaqus post-processing, and the sample's vertical deformation (mm) was recorded.

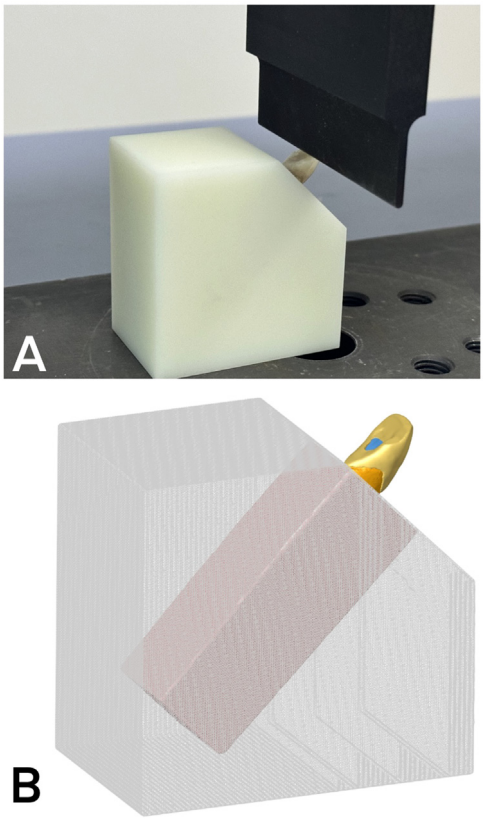

Fig. 4 – A, The load cell of the universal testing machine exerted pressure onto the lingual surface of the incisor. B, The assembly of the incisor model, the block model, and the testing base model.

The deformation of the sample under different pressures measured by the universal testing machine was paired with the deformation data simulated by FEA, and a Bland–Altman plot was generated using GraphPad Prism 10 (GraphPad Software, Boston, MA, USA).

Results

In Figure 5, the Bland–Altman analysis revealed that the errors in both measured and calculated deformation values

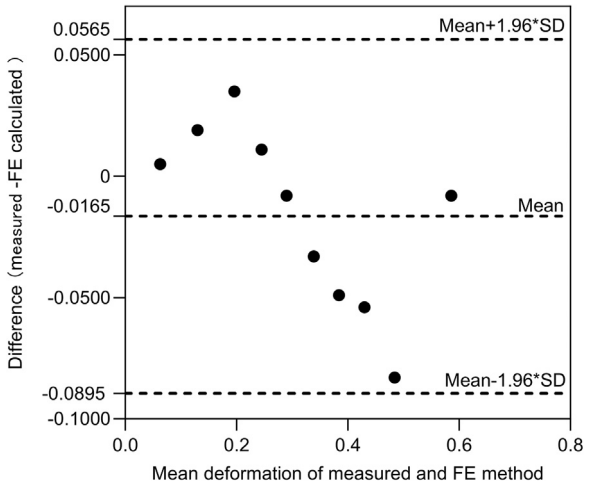

Fig. 5 – Bland–Altman plots for measured deformation with FE calculated deformation. The dotted lines show mean and 95% limits of agreement.

fell within the 95% limits of agreement, affirming the FEA validity.

The removed dentin volume and the removed pericervical dentin (PCD) volume in different models are shown in Table 2. The TAC models exhibit the highest volume of removed dental tissue, followed by the IAC models, CAC models, and CIAC models. The TAC models demonstrate the greatest extent of dental tissue removal in the cervical region, followed by the CAC, IAC, and CIAC models.

The distribution diagrams in Figure 6A and D, and Figure 7G and J illustrate the distribution of maximum principal stress and von Mises (VM) stress in the intact dentin model under the conditions of 250 N and 50 N. The highest values of both maximum principal stress and VM stress are concentrated in the cervical region on the lingual and labial sides of the dental tissue, with a gradual decrease as it approaches the root canal region. The areas near the incisal and apical edges of the dental tissue model and the mesial and distal regions of the cervical area exhibit the lowest VM stress.

As shown in Table 2, the maximum tensile stress of the treated teeth is higher than that of the intact teeth. Under loads of 250 N and 50 N, the ranking of the maximum tensile stress in the cervical area exhibits similarity, highest in the TAC group, followed by the CAC, IAC, and CIAC groups. Regarding the apex region, the maximum tensile stress under the force of 250 N is highest in the IAC group, followed by the CAC, TAC, and CIAC groups. However, under the force of 50 N, the order of maximum tensile stress at the root apex changes, with the CAC group exhibiting the highest stress, followed by the TAC, IAC, and CIAC groups. Figure 6B and C, and Figure 7H and I illustrate the maximum principal stress distribution in the dental tissue at the CEJ and root apex. In the cervical and apical regions, the maximum principal stress exhibits tensile stress on the lingual side and compressive stress on the labial side. In the region near the root apex, the IAC and IT groups exhibit significantly lower maximum principal stress than the other 3 groups.

As shown in Table 2, the VM stress in the treated teeth is higher than in the intact teeth. The VM stresses under loads of 250 N and 50 N show consistent rankings for the TAC, CAC, IAC, and CIAC groups. The highest values are observed in the TAC group, followed by the CAC, IAC, and CIAC groups, both at the cervical area and the root apex. Figure 6E and F, and Figure 7K and L illustrate the distribution of VM stress in the dental tissue at the CEJ and root apex. In the cervical region, VM stress is mainly concentrated on the lingual side, close to the surface area. In the apical region, VM stress is concentrated on the labial and buccal sides, with the lowest values near the root canal region.

Discussion

The present study compared the effects of different access cavities on the biomechanical performance of incisors. Variations in the endodontic access cavity models considerably influenced the maximum VM stress and maximum principal stress along the dentin when exposed to occlusal force. Therefore, the null hypothesis was rejected.

The concept of a conservative access cavity, also known as a minimally invasive access cavity, is based on the idea that preserving more dental tissue can improve the mechanical performance of teeth.[30] Numerous studies have been conducted in recent years to investigate the effects of minimally invasive access cavities on root canal cleaning and shaping abilities and the fracture resistance of teeth.[18,31-35] However,

Table 2 – Results of the study models.

Applied Force	Outcome measure	IT	CIAC	IAC	CAC	TAC
	Removed dentin volume (mm^3)	0	6.73	12.25	8.85	21.11
	Removed PCD volume (mm^3)	0	3.16	6.01	6.30	15.42
250 N load	Max tensile MPS in the cervical area(MPa)	8.34	9.54	11.50	12.54	12.70
	Max tensile MPS in apical area(MPa)	3.10	3.50	4.67	4.50	4.47
	Max VM stress in the cervical area(MPa)	7.85	8.93	10.02	11.35	11.41
	Max VM stress in the apical area(MPa)	3.55	3.81	4.68	5.08	5.19
50 N load	Max tensile MPS in the cervical area(MPa)	1.67	1.92	2.34	2.51	2.76
	Max tensile MPS in apical area(MPa)	0.62	0.70	0.93	0.90	0.97
	Max VM stress in the cervical area(MPa)	1.57	1.77	2.00	2.43	2.48
	Max VM stress in the apical area(MPa)	0.71	0.76	0.94	1.02	1.13

CAC, conservative access cavity; CIAC, conservative incisal access cavity; IAC, incisal access cavity; IT, intact tooth; MPS, maximum principal stress; PCD, pericervical dentin; TAC, traditional access cavity; VM, von Mises.

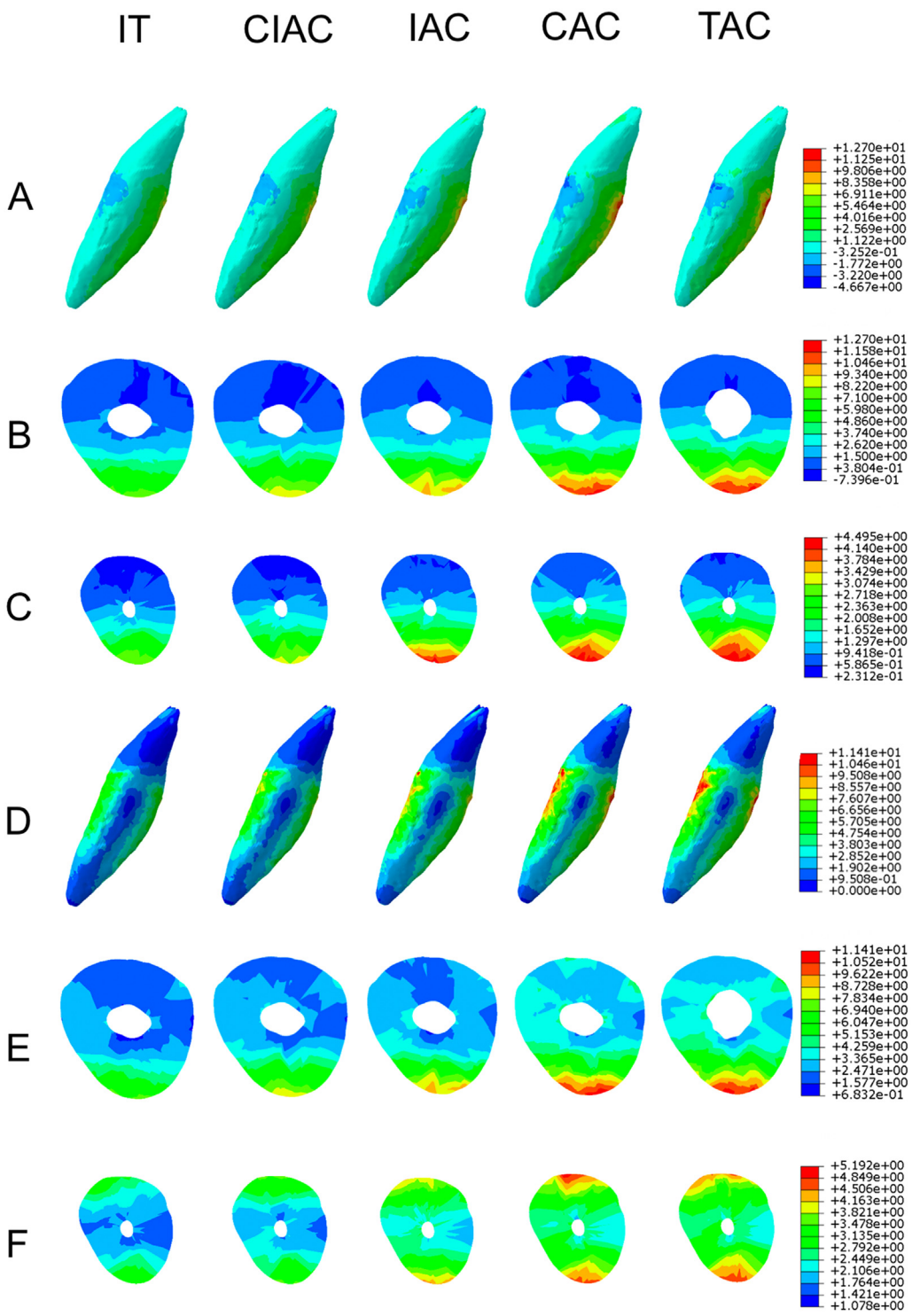

Fig. 6 – The distributions of the maximum principal stress under 250 N on the A, Lateral view of the dentin model. B, The transverse cross-section in the cervical area. C, The transverse cross-section in the apical area. The distributions of the von Mises stress on the D, Lateral view of the dentin model. E, The transverse cross-section in the cervical area. F, The transverse cross-section in the apical area.

most of the conservative design studies have focused on reducing the size of the access cavity and have mainly been performed on molars with complex canal structures, and the conclusions drawn have not been consistent. Additionally, using a conservative access cavity increases the demands for specific equipment, lighting, and skills and can increase the complexity of the procedure to some extent. Therefore, solid research results are needed to support the application of this approach in clinical practice. This study aims to experimentally compare the impact of various root canal access cavity

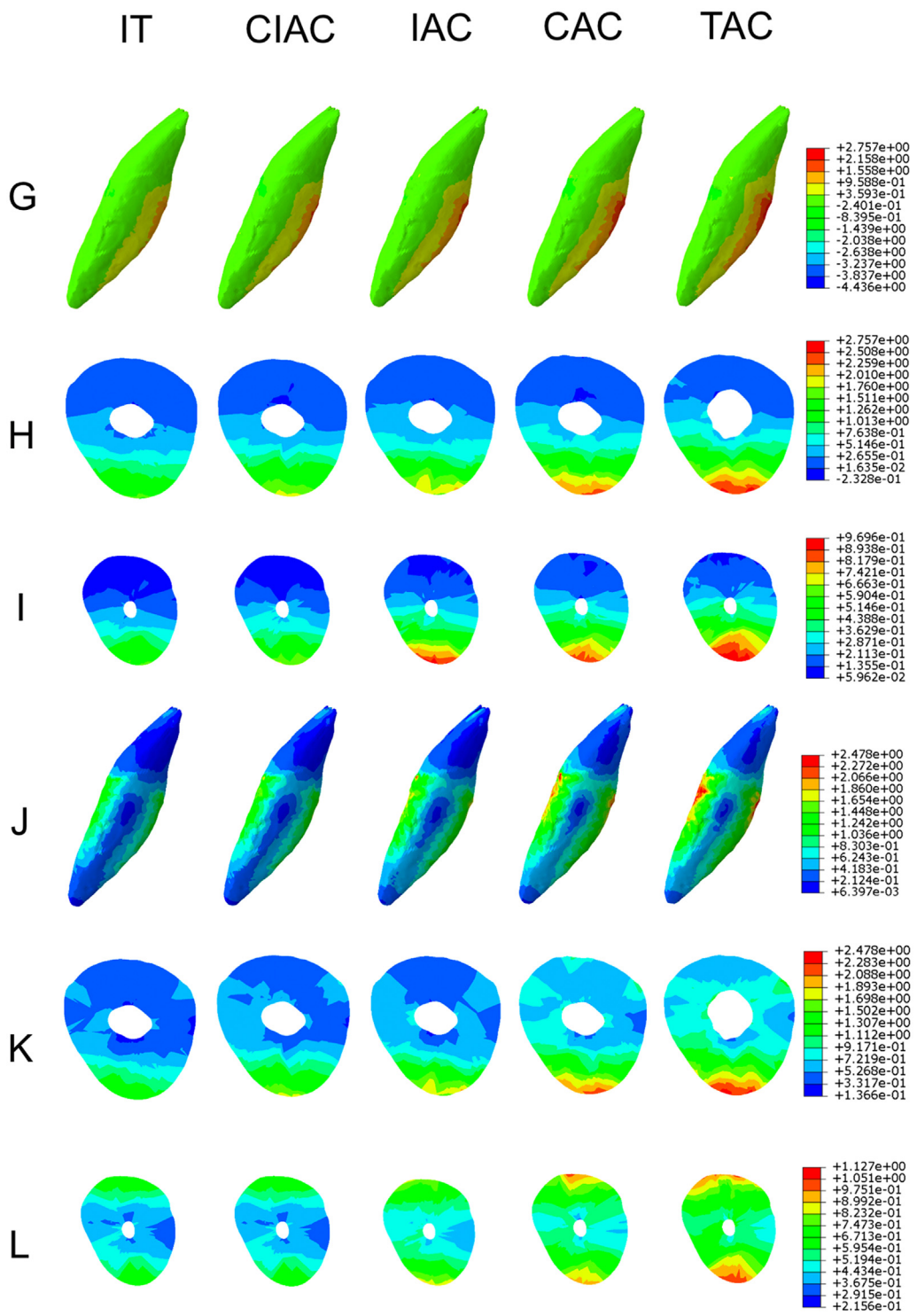

Fig. 7 – The distributions of the maximum principal stress under 50 N on the G, Lateral view of the dentin model. H, The transverse cross-section in the cervical area. I, The transverse cross-section in the apical area. The distributions of the von Mises stress on the J, Lateral view of the dentin model. K, The transverse cross-section in the cervical area. L, The transverse cross-section in the apical area.

approaches on the resistance to incisor fractures. The goal is to provide clinicians with insights for adopting more effective methods in incisor root canal treatments, enhancing the post-treatment strength of patients' teeth and thereby improving prognosis.

Many ex-vivo experiments have been performed using a universal testing machine to test the fracture resistance of teeth. However, because the experimental methods vary, with some teeth filled and others unfilled, or some teeth undergoing cyclic loading while others do not, the uniformity

of the experimental conditions could be better. In contrast, the use of FEA provides several advantages, including the ability to model teeth using high-resolution micro-CT scans and design different access cavities on the same tooth model, simulate uniform loading conditions, and analyse stress distribution and maximum stress in teeth, thus minimizing differences between teeth and errors caused by variations in experimental procedures.

In this study, we added the IAC pathway, which does not involve the conservative portion of the CAC pathway but instead moves the access point towards the incisal edge to create an oval-shaped opening similar to the second pathway used in G. Mannan's experiment.[16] One of the objectives of this study was to use a standardised experimental design to compare the differences in preserving the fracture resistance of the incisor between using the IAC pathway and the more complicated CIAC pathway.

The findings of the current investigation were assessed using VM stress and the maximum principal stress analysis. VM stress serves as a failure criterion, indicating energy distribution within the structure. Maximum principal stress differentiates between tensile stress (positive values) and compressive stress (negative values). Dental materials and structures typically exhibit high compressive strength but tend to be brittle when subjected to tensile stress.[36] Consequently, maximum principal stress enables the identification of vulnerable areas within the structure that are more susceptible to failure due to tensile stress.[37] When evaluating root-filled teeth, maximum principal stress proves to be a highly effective criterion for pinpointing potential critical points of failure within the dental structure.

The results demonstrate that the maximum principal stress and VM stress are concentrated in the cervical region of the tooth, indicating that this area is most vulnerable to fracture when subjected to biting pressure in the maxillary central incisor. The focal point of this study's analysis lies specifically within this region. Under the 250 N and 50 N loading conditions, the maximum VM stress and maximum principal stress in the cervical area of the dentin model follow the same pattern: TAC > CAC > IAC > CIAC. This indicates that the mechanical properties of teeth vary depending on the different access cavity approaches. Compared to untreated teeth, the fracture resistance of treated teeth deteriorates, especially when employing the traditional access method, which makes them more prone to fracture. The CIAC method exhibits the best resistance to flexural stress among the 4 approaches. Regarding the cervical area, the CAC group shows lower maximum principal stress and VM stress than the TAC group. Similarly, CIAC exhibits lower values than IAC. These findings suggest that adopting a conservative access approach can improve the fracture resistance of teeth. These findings align with previous studies conducted by Sarvaiya et al.[13] This may be attributed to the conservative access method preserving more of the fragile tooth cervical area by reducing the amount of dentin removal.

When comparing IAC to TAC, the maximum VM stress and maximum principal stress in the cervical region are lower for IAC. Similarly, when comparing CIAC to CAC, the maximum VM stress and maximum principal stress in the cervical region of the incisor are lower for CIAC. These results indicate that the fracture resistance of maxillary central incisors is superior when employing an incisal edge access approach compared to a lingual access approach.

The amount of dentin removal varies among the four access approaches, with TAC having the highest amount, followed by IAC, CAC, and CIAC. However, the sequence becomes TAC > CAC > IAC > CIAC when considering dentin removal, specifically in the cervical region. The differences in the amount of dentin removal correspond to the fracture resistance results of the tooth models in the cervical region. In other words, the TAC group with the most PCD removal exhibits the poorest mechanical strength. In contrast, the CIAC group with the most minor PCD removal demonstrates the best mechanical strength. The IAC group employs an incisal access approach with less PCD removal than the conservative CAC group. This can be attributed to the incisal access approach starting at the incisal edge, resulting in the systematic removal of more dentin near the edge of the crown and reducing the amount of dentin removal in the tooth cervical region. The preservation of tooth structure in the cervical area is crucial for preventing fractures under occlusal forces and ensuring the long-term viability of endodontically treated teeth.[30] This may explain why the IAC group exhibits even better flexural resistance despite not employing a conservative access approach than the CAC group.

The traditional and conservative pathway's access point is situated at the central position of the lingual surface of the dental crown. When performing the TAC and CAC access, extending the entry point from the lingual side to the root canal results in the removal of a significant amount of dentin at the cervical area of the incisor. In contrast, locating the entrance point for the incisal access cavity at the incisal edge and extending it along the longitudinal axis of the incisor towards the root canal avoids unnecessary removal of pericervical dentin tissue. Another advantage of this incisal access cavity is the improved accessibility from the coronal portion of the root to the apex. This incisal-shifted access facilitates a broader surface area of the root canal walls to be reached by instruments such as Gates Glidden Drills and K-files.[16] Therefore, IAC and CIAC may have the ability to protect patients' teeth better and improve treatment outcomes in clinical situations.

This study is the first application of FEA to compare the 4 different access cavities of incisors, serving as a reference for choosing appropriate clinical procedures. In this study, the model of the alveolar bone around the incisor was configured as a cylindrical structure with completely bounded cortical and cancellous bone models. This aimed to provide a standardised, simplified model, facilitate consistent force application directions across different models, and enable comparison between experiments. Similar to our experiment, previous FEA studies have also distinguished cortical and cancellous bone models or cylindrical bone model designs.[18,31,35,38] This commonly used simplification can be considered a limitation of this study, as the bone model utilised in FEA differs from the actual morphology of the maxillary bone. Another limitation of this study is that using a standardised thickness for the periodontal ligament throughout the root may not fully represent the complex nature of the periodontal ligament in

reality. Future investigations could also evaluate the influence of access cavity designs on the cyclic fatigue life of incisors using fatigue testing machine.

Within the limitations of this study, the TAC group had the highest level of VM stress and tensile stress in the cervical area of incisor models, followed by the CAC, IAC, and CIAC groups. The conservative access cavities minimise the extent of dentin removal from the cervical region, protecting the mechanical behaviour of the incisor. Moving the access cavity entry point to the incisal edge also improves the fracture resistance of the incisor.

Data availability statement

The supporting data for the results of this research are available upon request from the corresponding author via email.

Ethical approval

The research obtained ethical clearance from the Ethics Committee of the Hospital of Stomatology at Jilin University, under protocol number 202309. It was conducted in strict accordance with the World Medical Association's Declaration of Helsinki, specifically adhering to the 2002 version. All methods involving human subjects were carried out following the ethical standards set by the Ethics Committee of Jilin University. Prior to their inclusion in the study, all participants were provided with comprehensive oral and written information about the study procedures, following which they provided their formal consent by signing an officially approved consent document.

Author contributions

Yujiang Liu, Xinyao Huang, Haoyu Ke, and Shufen Sun conceptualised the study. Yujiang Liu, Xinyao Huang, Haoyu Ke, and Shufen Sun contributed to the methodology. Yujiang Liu, Xinyi Song, and Xinmeng Huang contributed to the software. Yujiang Liu, Haoyu Ke, Xinmeng Huang, and Shufen Sun validated the study. Yujiang Liu, Xinyi Song, and Shufen Sun contributed to the formal analysis. Yujiang Liu, Xinyao Huang, Haoyu Ke, Xinmeng Huang, and Shufen Sun contributed to the investigation, resources, data curation, writing – original draft preparation, and writing – review and editing. All authors have read and agreed to the published version of the manuscript.

Conflict of interest

None disclosed.

Funding

This research did not receive funding from any specific grant provided by public, commercial, or not-for-profit entities.

REFERENCES

1. Clark D, Khademi J. Modern molar endodontic access and directed dentin conservation. Dent Clin North Am 2010;54 (2):249–73. doi: 10.1016/j.cden.2010.01.001.
2. Corsentino G, Pedullà E, Castelli L, et al. Influence of access cavity preparation and remaining tooth substance on fracture strength of endodontically treated teeth. J Endod 2018;44 (9):1416–21. doi: 10.1016/j.joen.2018.05.012.
3. Lima CO, Barbosa AFA, Ferreira CM, et al. Influence of ultraconservative access cavities on instrumentation efficacy with XP-endo Shaper and Reciproc, filling ability and load capacity of mandibular molars subjected to thermomechanical cycling. Int Endod J 2021;54(8):1383–93. doi: 10.1111/iej.13525.
4. Santosh SS, Ballal S, Natanasabapathy V. Influence of minimally invasive access cavity designs on the fracture resistance of endodontically treated mandibular molars subjected to thermocycling and dynamic loading. J Endod 2021;47 (9):1496–500. doi: 10.1016/j.joen.2021.06.020.
5. Krishan R, Paqué F, Ossareh A, Kishen A, Dao T, Friedman S. Impacts of conservative endodontic cavity on root canal instrumentation efficacy and resistance to fracture assessed in incisors, premolars, and molars. J Endod 2014;40(8):1160–6. doi: 10.1016/j.joen.2013.12.012.
6. Rover G, Belladonna FG, Bortoluzzi EA, De-Deus G, Silva EJNL, Teixeira CS. Influence of access cavity design on root canal detection, instrumentation efficacy, and fracture resistance assessed in maxillary molars. J Endod 2017;43(10):1657–62. doi: 10.1016/j.joen.2017.05.006.
7. Silva EJNL, Pacheco PT, Pires F, Belladonna FG, De-Deus G. Microcomputed tomographic evaluation of canal transportation and centring ability of ProTaper Next and Twisted File Adaptive systems. Int Endod J 2017;50(7):694–9. doi: 10.1111/iej.12667.
8. Silva EJNL, Pinto KP, Ferreira CM, et al. Current status on minimal access cavity preparations: a critical analysis and a proposal for a universal nomenclature. Int Endod J 2020;53 (12):1618–35. doi: 10.1111/iej.13391.
9. Rover G, Lima CO, Belladonna FG, et al. Influence of minimally invasive endodontic access cavities on root canal shaping and filling ability, pulp chamber cleaning and fracture resistance of extracted human mandibular incisors. Int Endod J 2020;53 (11):1530–9. doi: 10.1111/iej.13378.
10. Santos Miranda ARL, Moura JDM, Calefi PHS, et al. Influence of conservative endodontic access cavities on instrumentation of oval-shaped straight root canals. Int Endod J 2022;55 (1):103–12. doi: 10.1111/iej.13635.
11. Yahata Y, Masuda Y, Komabayashi T. Comparison of apical centring ability between incisal-shifted access and traditional lingual access for maxillary anterior teeth. Aust Endod J 2017;43(3):123–8. doi: 10.1111/aej.12190.
12. Mauger MJ, Waite RM, Alexander JB, Schindler WG. Ideal endodontic access in mandibular incisors. J Endod 1999;25(3):206–7. doi: 10.1016/S0099-2399(99)80143-5.
13. Sarvaiya UP, Rudagi K, Joseph J. A comparative evaluation of the effect of different access cavity designs on root canal instrumentation efficacy and resistance to fracture assessed on maxillary central incisors: an in vitro study. J Conserv Dent JCD 2020;23(6):609–14. doi: 10.4103/JCD.JCD_600_20.
14. Zillich RM, Jerome JK. Endodontic access to maxillary lateral incisors. Oral Surg Oral Med Oral Pathol 1981;52(4):443–5. doi: 10.1016/0030-4220(81)90347-9.
15. LaTurno SA, Zillich RM. Straight-line endodontic access to anterior teeth. Oral Surg Oral Med Oral Pathol 1985;59(4):418–9. doi: 10.1016/0030-4220(85)90069-6.
16. Mannan G, Smallwood ER, Gulabivala K. Effect of access cavity location and design on degree and distribution of

instrumented root canal surface in maxillary anterior teeth: access cavities and instrumented surface in root canals. Int Endod J 2001;34(3):176–83. doi: 10.1046/j.1365-2591.2001.00359.x.
17. Nanci A, Bosshardt DD. Structure of periodontal tissues in health and disease. Periodontol 2000;40(1):11–28. doi: 10.1111/j.1600-0757.2005.00141.x.
18. Fu Y, Zhang L, Gao Y, Huang D. A comparison of volume of tissue removed and biomechanical analysis of different access cavity designs in 2-rooted mandibular first molars: a multi-sample 3-dimensional finite element analysis. J Endod 2022;48(3):362–9. doi: 10.1016/j.joen.2021.12.007.
19. Katranji A, Misch K, Wang H. Cortical bone thickness in dentate and edentulous human cadavers. J Periodontol 2007;78(5):874–8. doi: 10.1902/jop.2007.060342.
20. Peyton FA, Mahler DB. Physical properties of dentin. J Dent Res 1952;31(3):366–70. doi: 10.1177/00220345520310031401.
21. Farah JW, Craig RG, Meroueh KA. Finite element analysis of three- and four-unit bridges. J Oral Rehabil 1989;16(6):603–11. doi: 10.1111/j.1365-2842.1989.tb01384.x.
22. Gale MS, Darvell BW. Thermal cycling procedures for laboratory testing of dental restorations. J Dent 1999;27(2):89–99. doi: 10.1016/S0300-5712(98)00037-2.
23. Friedman CM, Sandrik JL, Heuer MA, Rapp GW. Composition and mechanical properties of gutta-percha endodontic points. J Dent Res 1975;54(5):921–5. doi: 10.1177/00220345750540052901.
24. Eraslan Ö, Eraslan O, Eskitaşcıoğlu G, Belli S. Conservative restoration of severely damaged endodontically treated premolar teeth: a FEM study. Clin Oral Investig 2011;15(3):403–8. doi: 10.1007/s00784-010-0397-7.
25. Borges Radaelli MT, Idogava HT, Spazzin AO, Noritomi PY, Boscato N. Parafunctional loading and occlusal device on stress distribution around implants: a 3D finite element analysis. J Prosthet Dent 2018;120(4):565–72. doi: 10.1016/j.prosdent.2017.12.023.
26. Cantrell JT, Rohde S, Damiani D, et al. Experimental characterization of the mechanical properties of 3D-printed ABS and polycarbonate parts. Rapid Prototyp J 2017;23(4):811–24. doi: 10.1108/RPJ-03-2016-0042.
27. Bucchi C, Marcé-Nogué J, Galler KM, Widbiller M. Biomechanical performance of an immature maxillary central incisor after revitalization: a finite element analysis. Int Endod J 2019;52(10):1508–18. doi: 10.1111/iej.13159.
28. Kumagai H, Suzuki T, Hamada T, Sondang P, Fujitani M, Nikawa H. Occlusal force distribution on the dental arch during various levels of clenching. J Oral Rehabil 1999;26(12):932–5. doi: 10.1046/j.1365-2842.1999.00473.x.
29. Eram A, Zuber M, Keni LG, et al. Finite element analysis of immature teeth filled with MTA, Biodentine and Bioaggregate. Comput Methods Programs Biomed 2020;190:105356. doi: 10.1016/j.cmpb.2020.105356.
30. Ng CCH, Dumbrigue HB, Al-Bayat MI, Griggs JA, Wakefield CW. Influence of remaining coronal tooth structure location on the fracture resistance of restored endodontically treated anterior teeth. J Prosthet Dent 2006;95(4):290–6. doi: 10.1016/j.prosdent.2006.02.026.
31. Nawar NN, Kataia M, Omar N, Kataia EM, Kim HC. Biomechanical behavior and life span of maxillary molar according to the access preparation and pericervical dentin preservation: finite element analysis. J Endod 2022;48(7):902–8. doi: 10.1016/j.joen.2022.03.013.
32. Wang Q, Liu Y, Wang Z, et al. Effect of access cavities and canal enlargement on biomechanics of endodontically treated teeth: a finite element analysis. J Endod 2020;46(10):1501–7. doi: 10.1016/j.joen.2020.06.013.
33. Elkholy MMA, Nawar NN, Ha WN, Saber SM, Kim HC. Impact of canal taper and access cavity design on the life span of an endodontically treated mandibular molar: a finite element analysis. J Endod 2021;47(9):1472–80. doi: 10.1016/j.joen.2021.06.009.
34. Liu Y, Liu H, Fan B. Influence of cavity designs on fracture behavior of a mandibular first premolar with a severely curved h-shaped canal. J Endod 2021;47(6):1000–6. doi: 10.1016/j.joen.2021.03.012.
35. Zhang Y, Liu Y, She Y, Liang Y, Xu F, Fang C. The effect of endodontic access cavities on fracture resistance of first maxillary molar using the extended finite element method. J Endod 2019;45(3):316–21. doi: 10.1016/j.joen.2018.12.006.
36. Chai H, Lee JJW, Kwon JY, Lucas PW, Lawn BR. A simple model for enamel fracture from margin cracks. Acta Biomater 2009;5(5):1663–7. doi: 10.1016/j.actbio.2008.11.007.
37. Veríssimo C, Simamoto Júnior PC, Soares CJ, Noritomi PY, Santos-Filho PCF. Effect of the crown, post, and remaining coronal dentin on the biomechanical behavior of endodontically treated maxillary central incisors. J Prosthet Dent 2014;111(3):234–46. doi: 10.1016/j.prosdent.2013.07.006.
38. Baniasadi M, Darijani H, Parirokh M, Hamze F. Evaluating the effect of oblique ridge conservation on stress distribution in an endodontically treated maxillary first molar: a finite element study. J Endod 2021;47(3):500–8. doi: 10.1016/j.joen.2020.12.010.